

Imprint of large-scale atmospheric transport patterns on sea-salt records in northern Greenland ice cores

Hubertus Fischer

Alfred Wegener Institute for Polar and Marine Research, Bremerhaven, Germany

Abstract. The decadal to interannual variability of sea-salt aerosol concentrations in northern Greenland ice cores is investigated and contrasted to meteorological reanalysis data over the time span 1959–1993. Correlation analysis with average data on sea level pressure and geopotential height at the 500 mbar level identifies the eastern and northeastern Pacific region as the most important center of action responsible for variations in sea-salt aerosol export onto the Greenland ice sheet which is related to the Pacific/North American teleconnection pattern. The Atlantic region, however, appears to be of secondary importance only. Correlation coefficients are highest during the first quarter of the year but also significant for annual pressure data, explaining ~20% of the sea-salt variance in the ice cores. Furthermore, higher storm activity in the Pacific center of action, as well as in the northern Atlantic, leads to higher sea-salt concentrations in northern Greenland, explaining about 40% and 17% of the ice core variance. A 30% increase during the nineteenth century in a 600 year sea-salt record from northeastern Greenland may be interpreted, at least in part, as an enhancement of sea-salt export from the Pacific region during that time.

1. Introduction

During recent years, studies of the natural climate variability on decadal and centennial timescales have gained great importance in order to detect and quantify a potential anthropogenic climate change. In this regard the identification of large-scale teleconnection patterns, their temporal variability, and driving forces appears to be most important in detecting a possible change in recent atmospheric circulation [Corti *et al.*, 1999]. These efforts, however, are impaired by the coverage of meteorological data which is most often limited both in time and in space. Reliable long-term instrumental records, which allow quantification of the natural preindustrial climate variability and its ongoing change in the course of the twentieth century, exist only for a few locations of the globe [e.g., Bradley and Jones, 1992]. Climatologists have tried to extend the temporal coverage [Mann *et al.*, 1998] by compiling natural climate archives such as tree rings, corals, sea and lake sediments, as well as polar ice cores.

In this context, ice core records offer a most abundant, high-resolution archive of climate variability over the last 500–1000 years. They represent a passive recorder of climatic and environmental parameters such as local condensation temperature [e.g., Clausen *et al.*, 1988; Fischer *et al.*, 1998a; Johnsen *et al.*, 1992; Petit *et al.*, 1999] and snow accumulation [Alley *et al.*, 1993] on the ice sheets, natural and anthropogenic aerosol load of the atmosphere [e.g., Clausen *et al.*, 1995; Fischer *et al.*, 1998c; Hansson, 1994; Mayewski *et al.*, 1990, 1994], as well as atmospheric concentrations of greenhouse gases [e.g., Barnola *et al.*, 1995; Chappellaz *et al.*, 1993; Etheridge *et al.*, 1998]. Furthermore, great progress has recently been made in tracing the imprint of the North Atlantic Oscillation pattern in accumulation and isotopic records from Greenland ice cores [Appenzeller *et al.*, 1998; White *et al.*, 1997].

Thus far, only limited use has been made in this respect from aerosol records in polar ice cores, although such records are per se reflecting large-scale atmospheric transport patterns because both Greenland and Antarctica are essentially free of any significant

aerosol sources. To identify the most significant aerosol source areas and transport pathways responsible for aerosol concentrations in polar ice sheets, several approaches can be taken. First, they can be deduced from air mass back trajectory studies [e.g., Kahl *et al.*, 1997]. However, trajectory studies usually do not take precipitation into account, which may substantially deplete the atmospheric aerosol load during air mass transport. A second approach are studies on the isotopic composition of aerosol samples. For example, such an isotopic study on mineral dust particles by Svensson *et al.* [2000] identified Asian desert regions as the primary dust source dust for Greenland during the Last Glacial Maximum. While isotopic studies allow for an independent source apportionment, they give no insight into the transport pathways of the aerosol from the source to the point of deposition on the ice sheet and are not feasible for aerosol species, which isotopically show no distinct sources such as sea-salt aerosol.

In this study, another approach is followed to investigate the potential of ice core records as a reliable archive of temporal variations in atmospheric circulation based on the coherent inter-annual variability in regionally representative ice core records and meteorological reanalysis data. A similar approach has been recently applied on a single ice core from western Antarctica by Kreutz *et al.* [2000]. In the following, source regions and large-scale atmospheric circulation patterns relevant for the northern Greenland ice sheet are investigated by means of an empirical correlation analysis between reanalysis data compiled by the National Centers for Environmental Prediction (NCEP) and chemical ice core records from northern Greenland [Fischer *et al.*, 1998c] over the time span 1959–1993.

2. Methods

Ice cores, for this study, were drilled during the North Greenland Traverse (NGT) performed by the Alfred Wegener Institute during the years 1993–1995. Here two ice cores located in the climatologically homogeneous northeastern outflow region of the Greenland ice sheet (B18: 76°37'N, 36°24'W; B21: 80°00'N, 41°08'W) will be used. The cores have been subsampled in seasonal resolution (~4–10 samples per annual layer) over the time span 1959–1992 and 1960–1993 for B18 and B21, respec-

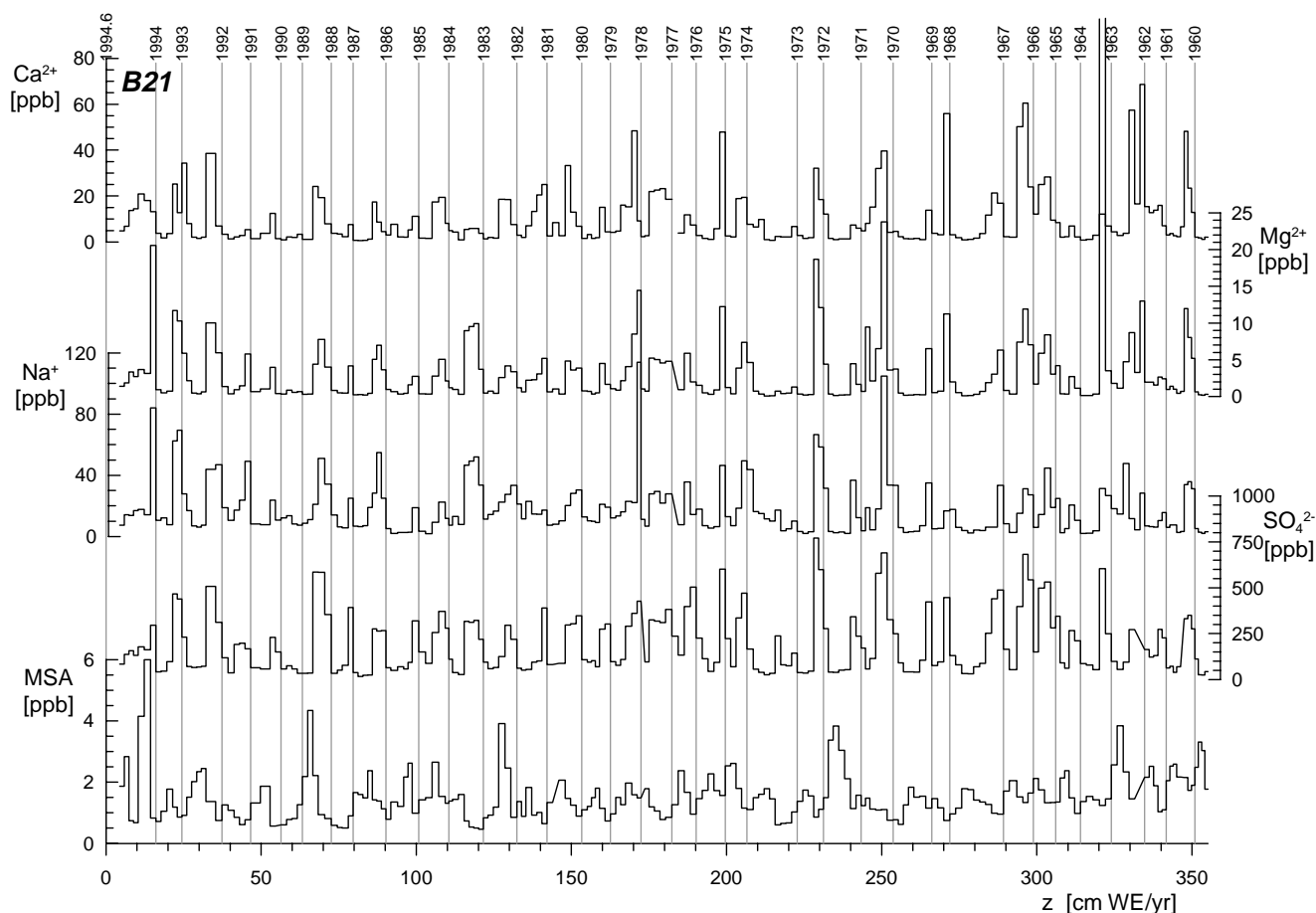


Figure 1. High-resolution ice core records of the ionic components Ca^{2+} , Mg^{2+} , Na^{+} , SO_4^{2-} and MSA in core B21 versus depth z in centimeters of water equivalent (WE) per year. Also indicated are the breakpoints of individual years for the time span 1960–1993.

tively, using contamination-free sampling protocols [Fischer, 1997]. Additionally, coarse resolution samples (3–4 years/sample for B18 and 1–2 years/sample for B21) were taken covering the last six centuries. Samples were ion chromatographically analyzed for major and trace ions at the Institute for Environmental Physics, University of Heidelberg [Fischer *et al.*, 1998b]. In the following, Na^{+} concentrations will be discussed in detail. In the case of Na^{+} the overall accuracy of the ion chromatographic measurements is 5–10% dependent on the concentration of the samples. Na^{+} is considered to represent essentially sea-salt aerosol concentrations. This assumption is supported by a pre-industrial $\text{Cl}^{-}/\text{Na}^{+}$ ratio very close to that of seawater. A small preindustrial Cl^{-} surplus of 3 ppb and 0 ppb has been found in cores B21 and B18, respectively. Thus any substantial Na^{+} contribution from other sodium sources is very unlikely. Instead, excess Cl^{-} in the ice may be attributed to acid-induced volatilization of HCl from sea-salt particles, volcanic emissions, or organic HCl sources such as CH_3Cl [Legrand and Delmas, 1988]. For the last few decades, significantly higher excess Cl^{-} concentrations are found in cores B18 and B21. These are most likely due to anthropogenic emissions, which either directly (by HCl emission) or indirectly (by acidification of the atmosphere) increase the excess Cl^{-} concentration in the atmosphere.

Absolute dating is most crucial for a correlation analysis because adding or missing only a single year will lead to a systematic error which depreciates the conclusions drawn from the correlation with meteorological parameters completely. To minimize the risk of such a misdating, a multitracer dating approach was followed using a suite of chemical tracers (SO_4^{2-} , Na^{+} , Mg^{2+} , Ca^{2+} , and methane

sulfonic acid (MSA)). All chemical components showed pronounced seasonal cycles, as illustrated in Figure 1. These cycles are in general agreement with previous results from other regions on the Greenland ice sheet [Beer, 1991; Fischer and Wagenbach, 1996; Steffensen, 1988]. Na^{+} showed a clear concentration maximum in midwinter relative to $\delta^{18}\text{O}$. Ca^{2+} , which is mainly influenced by mineral dust aerosol, and SO_4^{2-} , which is nowadays governed by anthropogenic sulfur sources, peak a little later in late winter/early spring. Mg^{2+} showed peak concentrations coincident with both the Na^{+} and the Ca^{2+} peaks, reflecting both sea salt and mineral dust contributions. Again, MSA, being derived from marine biogenic sources, showed a less distinct maximum during summer. This species showed a substantial decrease in the seasonal amplitude with depth most likely due to postdepositional migration of MSA ions in the snowpack. As a primary dating parameter, SO_4^{2-} was used, showing the largest seasonal amplitude. Where SO_4^{2-} was in doubt, Na^{+} , Mg^{2+} , and Ca^{2+} were also considered, and in a third step, MSA was also taken into account. With this approach it appears to be possible to date the high-resolution records with an error better than 1 year over the period 1959–1993. An independent age check may be found by control years, defined by extraordinarily high sulfate concentrations due to volcanic eruptions. For the time period starting from the 1960s, detection of such years, however, is impaired by the very high seasonal amplitude of sulfate concentrations due to anthropogenic emissions. Additionally, exact timing of the maximum deposition of volcanic aerosols may be delayed by up to 1 year in the case of stratospheric transport of aerosol onto the Greenland ice sheet. Only in the case of Icelandic volcanoes can a direct influence be

safely assumed on sulfate firm levels in the same year as the eruption. With respect to these restrictions, very high concentrations in 1970 in Figure 1 can be unambiguously attributed to the eruption of Hekla (Iceland) in this year. In the years 1963 and 1965–1967 there exists a prominent sequence of rather high sulfate concentrations which may be related to the eruptions of Agung (Indonesia), Sheveluch (Kamchatka), Taal (Philippines), and Awu (Indonesia) in the years 1963–1966. Extending the dating down to the 1950s, using high-resolution Ca^{2+} and NH_4^+ measurements [Sommer, 1996], a most pronounced peak can be found in the coarse resolution SO_4^{2-} record in the year 1956. This can be unambiguously connected to the most prominent eruption of Bezymyanny (Kamchatka) in this year. In summary these results support an absolute dating of the cores down to 1970 and a maximum error of up to 1 year for previous years. To define ice core years as closely to calendar years as possible, breakpoints of individual years were set in the middle of the rising flank of the SO_4^{2-} peaks. From the thus defined intervals, annual water-weighted means were derived for correlation analysis using firm density measurements performed on the ice core segments in the field.

If chemical ice core records are believed to reliably archive atmospheric circulation patterns, a significant part of the variance in the records has to be connected to variations in meteorological parameters. Further variance can be introduced by the variability of aerosol and trace gas deposition, by glaciological processes like the sastrugi formation [Steffensen *et al.*, 1996] as well as from postdepositional changes like wind drift, migration in the snow-pack [Legrand *et al.*, 1996; Minikin *et al.*, 1994], or net loss via the gas phase as encountered for NO_3^- [Fischer *et al.*, 1998b]. Also, the somewhat arbitrary definition of breakpoints between individual years in the ice core record results in higher interannual variability. One criterion to select aerosol species, which are suited for a correlation analysis with meteorological data, is a significant coherence within different ice cores in a climatologically homogeneous region. For the northern Greenland cores B18 and B21, only Na^+ and SO_4^{2-} records revealed significant correlation coefficients between the two cores ($r \approx 0.6$, significantly different from zero on the 99% level). In the case of SO_4^{2-} this shared variance stems essentially from the anthropogenic trend in SO_4^{2-} concentrations over the last four decades. Accordingly, it is not primarily linked to atmospheric circulation patterns and is excluded from further analysis. This leaves only Na^+ reflecting interannual variations in long-range transport and/or source strength changes of sea-salt aerosol over the last three decades. The lower noise level of sea salt, compared to other aerosol species, reflects in part its specific character with respect to aerosol transport and deposition, which is intimately linked to large-scale cyclonic activity. This results in a codeposition of sea salt and water vapor onto the Greenland ice sheet.

3. Results and Discussion

3.1. Correlation Analysis

To reveal spatial patterns of meteorological parameters related to the production and/or transport of sea-salt aerosol, the annual records of Na^+ concentration in cores B18 and B21 were correlated with annual and seasonal means of sea level pressure (SLP), geopotential height at 500 mbar (GPH500), sea surface temperature, and wind speed derived from NCEP reanalysis data at each individual grid point north of 20°N . This analysis revealed a very patchy, insignificant correlation pattern for wind speed and sea surface air temperature, which did not allow to unambiguously connect Greenland Na^+ concentrations to certain regions. In return the lack of a clear correlation pattern in wind speed (see Plate 1c) suggests that variations in sea-salt aerosol source strength is not the primary parameter governing the variability in northern Greenland snow concentrations over the last few decades.

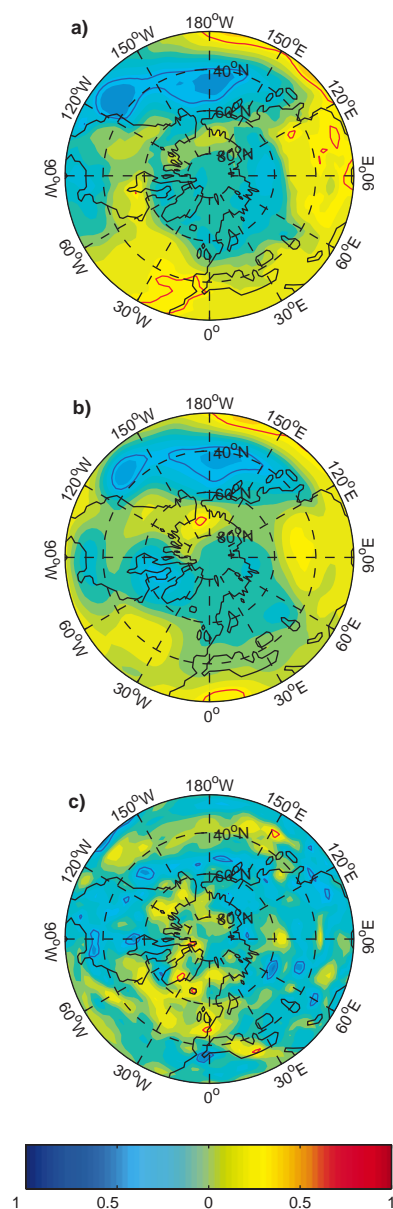


Plate 1. Correlation charts between annual means of Na^+ concentrations in core B21 and (a) sea level pressure, (b) geopotential height at the 500 mbar level, and (c) wind speed. Thick contours indicate the 95% significance level of the correlation coefficients.

Pointwise correlation of average annual SLP data and Na^+ concentrations in cores B21 and B18 showed distinct and significant correlation patterns that are most similar for both ice cores. This reveals a most pronounced anticorrelation pattern of annual Na^+ concentrations in northern Greenland ice and annual SLP (Plate 1a) in the northern and eastern Pacific region (local correlation coefficients $r < -0.45$, significant on the 99% level). This distribution will hereinafter be referred to as the Pacific correlation pattern (PCP). Comparison of sea-salt concentration with the time expansion coefficient of this pattern, which represents the projection of the pressure anomalies onto the regression map in the Pacific region ($20^\circ\text{--}90^\circ\text{N}$, $120^\circ\text{--}240^\circ\text{E}$), revealed an overall correlation coefficient of 0.46, explaining $\sim 20\%$ of the sea-salt variance in the ice core data. Besides the PCP a significant positive correlation of SLP with Na^+ ice core concentrations is found west off the African coast, which spreads westward across the Atlantic,

hereinafter referred to as the Atlantic correlation pattern (ACP). The fact that the independently dated cores B18 and B21 show essentially the same spatial distribution of the correlation coefficients may be regarded as an argument that the derived patterns are real. However, because of the intersite correlation of B18 and B21 this has to be expected, to some extent, anyhow. In the following the discussion will concentrate on the patterns derived from the sea-salt aerosol record in the most accurately dated core B21, taken as representative for both cores.

The question remains whether some misdating is affecting the correlation analysis. To test this, three-annual data sets for Na^+ and SLP as well as GPH500 were calculated which are only weakly affected by a single-year misdating. This data set revealed essentially the same correlation patterns as the annual data with higher correlation coefficients ($|r| > 0.6$), implying that no systematic dating error depreciates the conclusions. Also, subsets consisting of 17 randomly picked years showed essentially the same correlation patterns as the full data set with a variable significance of the correlation coefficients. Only in the case that the first consecutive 17 years of the record (the time interval 1960–1976) were selected, correlation coefficients in the northern Pacific region decreased to an insignificant -0.2 , while for the period 1977–1993, significant correlation coefficients < -0.5 were found. Whether this is due to a higher activity of the center of action in the latter half of the records or reflects an unlikely dating error at the bottom end of the core cannot be answered at this point.

Correlation analysis for the annual average in GPH500, representing pressure fluctuations in the free troposphere, revealed a similar center in the northern and eastern Pacific (Plate 1b) as the SLP data. The ACP shows up very weakly in the geopotential height data and is statistically significant only for the correlation with core B18 ($r > 0.4$, $p = 0.95$). No correlation is found with pressure data over the northern Atlantic, which because of its proximity to the Greenland ice sheet may be expected to be a prime source for sea-salt aerosol.

To narrow down seasonal variations in aerosol transport patterns, correlation analyses of the annual Na^+ records with seasonal pressure data were performed. This seasonal correlation analysis revealed the highest correlation coefficients of the PCP in the first quarter of the year with correlation coefficients < -0.5 in the eastern Pacific and variations in SLP and GPH500 explaining $\sim 30\%$ and 25% of the interannual variance in the sea-salt record. In the rest of the year the PCP vanishes. The seasonal picture over the Atlantic is less clear. In the third quarter of the year there exists a significant pattern for SLP with a significant positive correlation ($r > 0.55$) in a belt at $\sim 25^\circ\text{N}$ and an anticorrelation farther north. However, this pattern is not reflected in the geopotential height data, raising some doubt whether this correlation may be responsible for interannual variations in the background level of sea-salt concentrations in the northern Greenland ice core records.

Sea-salt transport is often linked to cyclonic activity, which is not necessarily represented in annual or seasonal averages in the pressure fields but should manifest itself in a higher variance in the pressure data. To test this, SLP and GPH500 were band-pass filtered (passing band 1–10 days) to reduce variance not related to storm activity. Subsequently, the variance of the filtered data set was calculated for individual years and seasons. This filtered variance, representing a measure of storm activity for the respective time interval at each grid point, was pointwise correlated with the sea-salt ice core data. The result of this analysis is plotted in Plates 2a and 2b for SLP and GPH500, respectively, showing significantly higher sea-salt concentrations in northern Greenland ice cores connected to higher storm activity mainly in the eastern but also in the western Pacific. Variations in the time expansion coefficient for the regression map between variance and ice core data in the Pacific region ($20^\circ\text{--}90^\circ\text{N}$, $120^\circ\text{--}240^\circ\text{E}$) explain $\sim 40\%$ of the variance in the Na^+ data in core B21. In contrast to the average pressure data a significant correlation is also revealed for

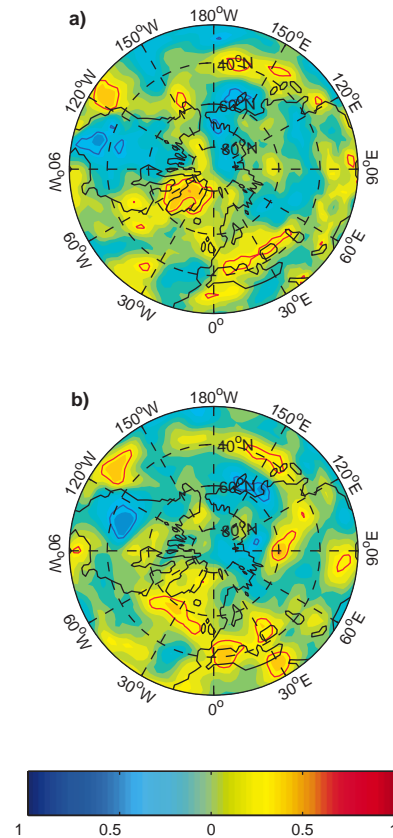


Plate 2. Correlation charts between annual means of Na^+ concentrations in core B21 and the variance of band-pass-filtered data in (a) SLP and (b) GPH500. Thick contours indicate the 95% significance level of the correlation coefficients

the annual variance in GPH500 in the northern Atlantic, which is related to the high storm activity in this region. Correlation of the time expansion coefficient for the Atlantic region ($20^\circ\text{--}90^\circ\text{N}$, $270^\circ\text{--}360^\circ\text{E}$) with the ice core data is 0.42 , explaining about 17% of the Na^+ variance in the ice core record.

In summary the outcome of the correlation analysis strongly supports Pacific pressure patterns to be most important for the average annual transport of sea-salt aerosol onto the northern Greenland ice sheet and probably into the whole Arctic basin. Here interannual pressure variations together with modulations in the storm activity in the eastern and northern Pacific lead to a higher sea-salt export onto the Greenland ice sheet with, on average, lower atmospheric pressure supporting higher storm activity in this region. Surprisingly, the Atlantic region appears to be of secondary importance only. While average pressure fields in the northern Atlantic are not significantly connected to sea-salt concentrations in northern Greenland ice cores, single storm events appear to be able to transport sea-salt aerosol from the northern Atlantic to the northern Greenland ice sheet. This result may be explained by the location of the drill sites east of the main ice divide, which blocks northeastern Greenland from the average airflow over the northern Atlantic region as also reflected in very low accumulation rates in this region. In a study by *Chen et al.* [1997] the importance for North Atlantic cyclones for the southern part of Greenland has been stressed. While they report crossings of cyclones from the west over the southern tip of Greenland, such a crossing in the central and especially northern part of the ice sheet should be strongly subdued. The result of this correlation analysis is also in qualitative agreement with trajectory studies performed for the central Greenland Summit region [*Kahl et al.*, 1997]. These

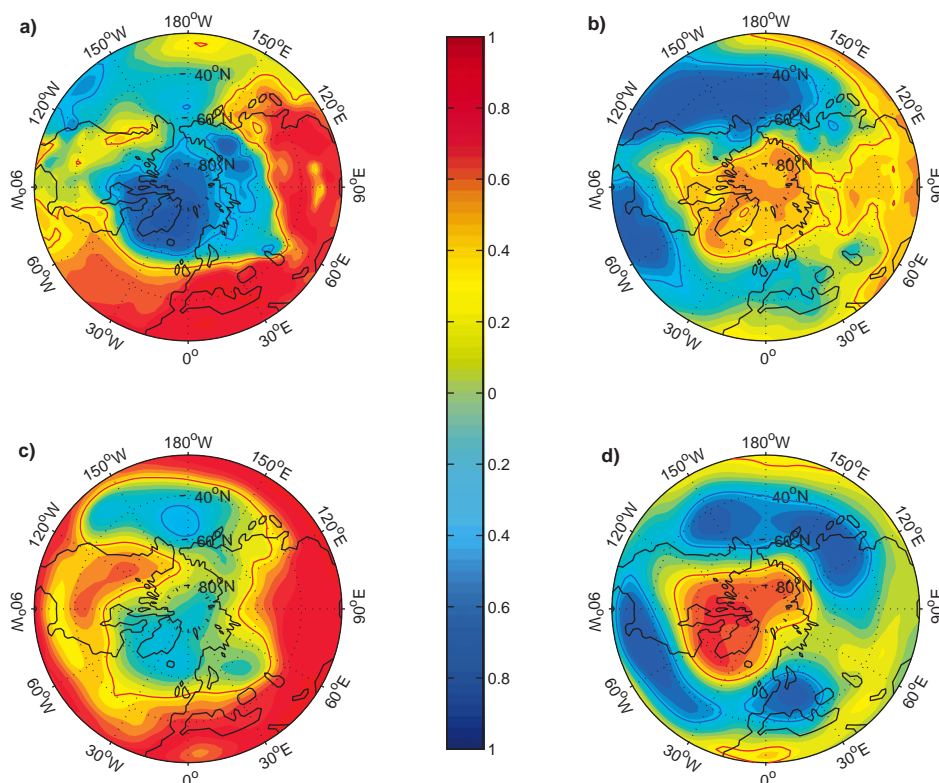


Plate 3. EOF analysis on annual means of SLP and GPH500 for grid points north of 20°N: (a) correlation between PC1 and SLP, (b) correlation between PC2 and SLP, (c) correlation between PC1 and GPH500, and (d) correlation between PC2 and GPH500. Thick contours indicate the 95% significance level of the correlation coefficients.

show that the large majority of 10 day back trajectories is pointed to the east (backward in time) from the Greenland Summit and either originates or crosses over the northern Pacific region during air mass transport. In contrast, only 4% of all trajectories for Summit originate in the North Atlantic [Kahl *et al.*, 1997]!

3.2. Teleconnection Patterns

The empirical correlation analysis above identifies important source regions and/or transport pathways for sea-salt aerosol deposited onto the northern Greenland ice sheet. The question arises whether these correlation patterns are connected to large-scale teleconnection patterns in atmospheric pressure data. In this case, sea-salt records could be used to reconstruct the temporal change of such teleconnections on longer timescales. To derive teleconnection patterns inherent in the pressure data, an empirical orthogonal function (EOF) analysis on the reanalysis data sets north of 20°N was performed (consistent with the studies by van Loon and Rogers [1978] and Wallace and Gutzler [1981] (herein-after referred to as WG81)). To be consistent with the correlation analysis, only the time span 1960–1993 was considered in the EOF analysis.

The results of this analysis for annual means in SLP are shown in Plates 3a and 3b as a correlation chart between the principal component (PC) and the pressure time series at the given grid point. The size of the correlation coefficients indicates how active the eigenvector is at a given grid point. The discussion in Plate 3 is confined to the first two EOFs, explaining 27% and 16% of the total variance in the data set (all other EOFs explain less than 10%). EOF1 reveals a rotation symmetrical pattern around the North Pole with a counterpart over the continental areas of North Africa and Eurasia. This feature can be recognized as an image of the Arctic Oscillation [Thompson and Wallace, 1998], with the anticorrelation pattern of EOF1 over the Atlantic region identified as a manifestation of the North Atlantic Oscillation pattern [Hur-

rell, 1995; van Loon and Rogers, 1978]. EOF2 shows a primary center of action over the northern and eastern Pacific in accordance with the PCP in section 3.1 but also in the southwestern part of the Atlantic. The Pacific center of action is counterbalanced by a center located over the pole and extending over the Asian continent and also into North America. It shares the most important features with the Pacific/North American (PNA) pattern defined in WG81.

The time series of EOF2 is correlated with the sea-salt record ($r > 0.3$ significant on the 90% level), which points to a link of sea-salt aerosol export with this pressure pattern. Note that although the given correlation coefficients are statistically significant, the shared variance of EOF2 and the Na^+ record in B21 is only about 10%, leaving plenty of room for depositional and postdepositional variance as well as other transport pathways to explain the remaining 90% of the variance in the sea-salt record. This strongly limits the quantitative representativeness of any long-term reconstruction of EOF2 on the basis of chemical ice core records from northern Greenland. EOF analysis has also been performed for GPH500, as illustrated in Plates 3c and 3d. In contrast to the SLP data, this reveals a less clear connection of large-scale EOF patterns with sea-salt export to the Greenland ice sheet. None of the two eigenvectors is significantly correlated with the sea-salt record, and EOF1 shows only a weak center of action over the northern Pacific. EOF2 reveals a rotation symmetrical center of action over the pole with two counterparts over the Atlantic and the western Pacific in good agreement with similar analyses in WG81.

In a second step, EOF analysis was performed on seasonally averaged pressure data north of 20°N. The eigenvectors for SLP showed essentially the same spatial patterns as for the annual data with the Pacific pattern being most pronounced in the first quarter of the year. The correlation coefficient of EOF2 with the Na^+ record for the first quarter of the year is 0.39 (significant on the $p = 95\%$ level) and explains 17% of the total variance in the SLP data.

Table 1. Correlation Coefficients of Annual Na^+ Concentrations in Core B21 With the Eastern Atlantic (EA) Pattern, the Pacific North American (PNA) Pattern, the Western Atlantic (WA) Pattern, the Western Pacific (WP) Pattern, the Eurasian (EU) Pattern and the North Atlantic Oscillation (NAO) Derived From Annual and Seasonal NCEP Reanalysis Data for the Time Span 1960–1993^a

Index	Annual	JFM	AMJ	JAS	OND
EA	(0.05)	(0.01)	(0.02)	(−0.04)	(0.10)
PNA	0.31	0.34	(0.22)	(−0.26)	(0.09)
WA	(−0.15)	(−0.06)	(0.03)	(0.24)	(−0.18)
WP	(−0.08)	(0.04)	(−0.02)	(0.19)	0.32
EI	(0.15)	(−0.01)	(0.31)	(0.01)	(0.08)
NAO	(0.18)	(0.13)	(0.05)	(−0.06)	(0.20)

^aCorrelation coefficients significant on the $p > 90\%$ level are without parentheses.

The seasonal EOF analysis for GPH500 revealed similar patterns as the annual data and, again, no significant correlation with our sea-salt record. This lack of correlation is in contrast to the direct correlation analysis in section 3.1, which revealed a significant correlation with GPH500 in the northern and eastern Pacific region. Obviously, the variability in GPH500 in the northeastern Pacific region is low compared to the variability in other regions of the Northern Hemisphere and is not represented by the first two eigenvectors in the EOF analysis.

EOF analysis is only able to define regions of hemispherically relevant variance in pressure data but does not reveal teleconnections in second-order indices, which are derived, for instance, by subtracting pressure data at one point on the hemisphere from the other. Such parameters, as for example the North Atlantic Oscillation index, may be more important for air mass transport because they are connected to real pressure gradients. In the following, correlation coefficients of the sea-salt record with Northern Hemispheric teleconnection indices as defined in WG81 for GPH500 are calculated, i.e., the eastern Atlantic (EA) pattern, the Pacific North American (PNA) pattern, the western Atlantic (WA) pattern, the western Pacific (WP) pattern, and the Eurasian (EU) pattern (for the definition of these indices, see WG81). Additionally, a North Atlantic Oscillation (NAO) index was derived from SLP according to $\text{NAO} = 0.5 (\text{SLP}(37.5^\circ\text{N}, 27.5^\circ\text{W}) - \text{SLP}(65^\circ\text{N}, 17.5^\circ\text{W}))$.

While WG81 defined their indices only for the winter season (December through February), here their formulas are applied both to annual and to seasonal data sets. The result of this analysis is

summarized in Table 1. For the first quarter of the year, which resembles the analysis done in WG81 most closely, a significant correlation ($r = 0.34$, $p = 95\%$) with the PNA was found. This is also the most important teleconnection pattern for sea-salt export in the annual data set (significant on the 90% level). Keeping in mind that the indices defined in WG81 may not be applicable for other seasons than winter, the correlation of the western Pacific pattern ($p > 90\%$) during the last quarter of the year might reflect the only other true connection with sea-salt export onto the Greenland ice sheet. In summary the correlation with teleconnection indices as well as the EOF analysis points to a connection of sea-salt aerosol concentrations in northern Greenland with the Pacific North American pattern. However, correlation coefficients are rather low. This has to be kept in mind when using sea-salt ice core records from northern Greenland for a long-term reconstruction of such patterns as intended in the following section.

3.3. Long-Term Sea-Salt Records

In Figure 2 the Na^+ record is plotted over the last 600 years derived from annual data of core B21, together with its long-term trend represented by a robust cubic spline. Dating of the core was accomplished by counting annual layers in continuous flow Ca^{2+} and NH_4^+ [Sommer, 1996] stratigraphies as well as high-resolution γ -ray attenuation density measurements [Wilhelms, 1996] together with identification of prominent volcanic horizons in the continuous sulfate [Fischer et al., 1998c] and electrical conductivity [Werner, 1995] records. Dating accuracy is estimated to be better than ± 3 years. As can be seen in Figure 2, the typical background Na^+ firm concentration in this low snow accumulation area is on the order of 10–15 ppb with single years in core B21 reaching concentrations as high as 30–90 ppb. The robust spline approximation, plotted in Figure 2, represents the long-term change in sea-salt concentrations and may be interpreted, at least in part, as a variation in the intensity of the northeastern Pacific center of action (PCP) in SLP and GPH500. As can be seen in Figure 2, there exists at least one pronounced period of systematically higher sea-salt concentrations over most of the nineteenth century in both northeastern Greenland ice cores. Additionally, there is a tendency of lower Na^+ concentration in the first half of the eighteenth century. On the basis of the correlation analysis the time intervals can be identified as periods of extremely high/low activity of the Pacific center of action, respectively. Using linear regression between the annual Na^+ record in core B21 and the time expansion coefficient of the SLP regression map for the Pacific region as well as for the PNA index defined in WG81, the right-hand scales in Figure 2

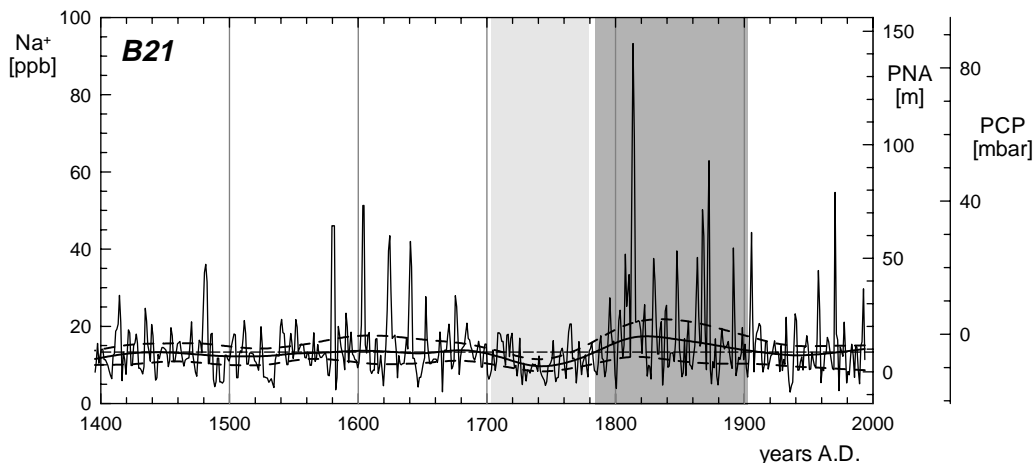


Figure 2. Long-term record of annual Na^+ concentration in core B21 over the last 600 years (thin line) together with a 25%, 50%, and 75% percentile robust spline (thick lines) (spline tension factor $q = 0.0001$ [Bloomfield and Steiger, 1983]). The right-hand scales indicate the respective changes in the Pacific North American (PNA) pattern index and in the time expansion coefficient of the Pacific correlation pattern (PCP).

were derived. With regard to the long-term trends in Figure 2 this suggests that the average annual SLP decreased by up to 10 mbar at the beginning of the nineteenth century. The PNA index increased by 15 m. On the basis of the outcome of the study, this would reflect a deepening of the pressure gradients in the free troposphere, hence a stronger geostrophic flow over the eastern Pacific region at that time leading to enhanced sea-salt export onto the northern Greenland ice sheet.

4. Conclusions

Using high-resolution data of sea-salt concentrations in two absolutely dated ice cores from northern Greenland together with reanalysis data of meteorological parameters, the most important centers of action responsible for long-term variations in sea-salt export onto the northern Greenland ice sheet could be identified. In summary, higher annual sea-salt concentrations are connected to lower atmospheric pressure and stronger cyclonic activity in the eastern and northern Pacific. However, other processes (e.g., depositional noise) are responsible for substantial parts of the variance in the annual ice core data. The pressure variability in the northeastern Pacific can be described, in part, by the Pacific North American teleconnection pattern. Similar to the modulation of the zonal flow related to the North Atlantic Oscillation, a deepened pressure gradient between the Aleutian Low and the North American High in the winter season should be able to intensify northward meridional flow and advection of sea-salt aerosol into the Arctic. Somewhat surprisingly, the influence of pressure variability over the Atlantic on sea-salt concentrations in northern Greenland seems to be limited on an annual to seasonal timescale. However, a significant effect by single storm events is supported by pressure variance data. This study also suggests an influence of different air masses for the southern and northern Greenland ice sheet with a higher influence of air masses originating over the Pacific farther north. Also, general circulation model results by Charles *et al.* [1994] show that the influence of Pacific water vapor sources increases in the north of Greenland, while the Atlantic influence decreases.

Special care has been taken in this study to test the robustness of the results, showing that snow chemistry records from single ice cores may be misleading, especially in low accumulation areas, because of the high depositional and postdepositional variability. For example, results of an equivalent analysis on mineral dust aerosol (as reflected in Ca^{2+} concentrations), would have led to erroneous correlation patterns dependent on which ice core would have been chosen. Only sea-salt concentrations in northern Greenland ice cores appear to be suited for the reconstruction of interannual variations in pressure patterns and aerosol transport. While this result is somewhat disappointing with respect to the reliability of ice cores in archiving interannual variations in aerosol transport, at least in low accumulation areas, one has to keep in mind that circulation changes acting on timescales of decades to millennia (such as the Little Ice Age, the Holocene climate optimum, glacial/interglacial changes, or rapid climate shifts such as the Dansgaard-Oeschger events) are distinctively reflected in ice core concentrations [Mayewski *et al.*, 1997; Mayewski, 1994; O'Brien *et al.*, 1995].

Similar regionally resolved studies in other regions of the Greenland ice sheet and in Antarctica will be the most important to derive spatial differences in the influence of circulation patterns relevant for different regions on the ice sheets. Here especially higher accumulation drill sites promise higher signal to noise ratios than in northern Greenland, but also regionally resolved studies may allow for improvement of the signal level. Extensive studies on the imprint of large-scale atmospheric transport patterns on aerosol concentrations in ice cores are currently under way within the presite survey for the upcoming deep drilling in Dronning Maud Land, Antarctica, within the European Project for Ice Coring

in Antarctica (EPICA). Here high-resolution continuous flow analyses on chemical species in the ice [Sommer *et al.*, 2000] promise new insights into the variability of atmospheric circulation over the southern Atlantic and Weddell Sea region.

Acknowledgments. This is a contribution to the research strategy project "Natural Climate Variations From 10,000 to the Present" by the Helmholtz association of German research centers, funded by the German Ministry for Education and Research. Chemical studies on the ice cores have been supported by Deutsche Forschungsgemeinschaft. The help of all people in the field and the lab is gratefully acknowledged. Thanks go to H. von Storch and coworkers, D. Wagenbach, and two referees for helpful comments on the manuscript. NCEP reanalysis data were kindly provided by the NOAA-CIRES Climate Diagnostics Center, Boulder, Colorado, United States. (at <http://www.cdc.noaa.gov/>)

References

- Alley, R. B., *et al.*, Abrupt increase in Greenland snow accumulation at the end of the Younger Dryas event, *Nature*, 362, 527–529, 1993.
- Appenzeller, C., T. F. Stocker, and M. Anklin, North Atlantic Oscillation dynamics recorded in Greenland ice cores, *Science*, 282, 446–449, 1998.
- Barnola, J. M., M. Anklin, J. Porcheron, D. Raynaud, J. Schwander, and B. Stauffer, CO_2 evolution during the last millennium as recorded by Antarctic and Greenland ice, *Tellus*, 47, 264–272, 1995.
- Beer, J., Seasonal variations in the concentrations of ^{10}Be , Cl^- , NO_3^- , SO_4^{2-} , H_2O_2 , ^{210}Pb , ^3H , mineral dust, and $\delta^{18}\text{O}$ in Greenland snow, *Atmos. Environ.*, 25(19), 899–904, 1991.
- Bloomfield, P., and W. L. Steiger, LAD spline fitting, in *Least Absolute Deviations: Theory, Applications and Algorithms*, pp. 131–168, Birkhauser Boston, Cambridge, Mass., 1983.
- Bradley, R. S., and P. D. Jones, *Climate since A.D. 1500*, Routledge, New York, 1992.
- Chappellaz, J., T. Blunier, D. Raynaud, J. M. Barnola, J. Schwander, and B. Stauffer, Synchronous changes in atmospheric CH_4 and Greenland climate between 40 and 8 kyr BP, *Nature*, 366, 443–445, 1993.
- Charles, C. D., D. Rind, J. Jouzel, R. D. Koster, and R. G. Fairbanks, Glacial-interglacial changes in moisture sources for Greenland: Influences on the ice core record of climate, *Science*, 263, 508–511, 1994.
- Chen, Q.-S., D.A. Bromwich, and L. Bai, Precipitation over Greenland retrieved by a dynamic method and its relation to cyclonic activity, *J. Clim.*, 10, 539–570, 1997.
- Clausen, H. B., N. S. Gundestrup, and S. J. Johnsen, Glaciological investigations in the Crete area: A search for a new deep drilling site, *Ann. Glaciol.*, 10, 10–15, 1988.
- Clausen, H. B., C. U. Hammer, J. Christensen, C. Schott Hvidberg, D. Dahl-Jensen, M. Legrand, and J. P. Steffensen, 1250 years of global volcanism as revealed by central Greenland ice cores, in *Ice Core Studies of Global Biogeochemical Cycles*, edited by R. J. Delmas, pp. 175–194, Springer-Verlag, Berlin, 1995.
- Corti, S., F. Molteni, and T. N. Palmer, Signature of recent climate change in frequencies of natural atmospheric circulation regimes, *Nature*, 398, 799–802, 1999.
- Etheridge, D. M., L. P. Steele, R. J. Francey, and R. L. Langenfelds, Atmospheric methane between 1000 A.D. and present: Evidence of anthropogenic emissions and climatic variability, *J. Geophys. Res.*, 103, 15,979–15,993, 1998.
- Fischer, H., and D. Wagenbach, Large-scale spatial trends in recent firm chemistry along an east-west transect through central Greenland, *Atmos. Environ.*, 30(19), 3227–3238, 1996.
- Fischer, H., Räumliche Variabilität in Eiskernzeitreihen Nordostgrönlands—Rekonstruktion klimatischer und luftchemischer Langzeitrends seit 1500 A.D., Institut für Umweltphysik, Universität Heidelberg, Heidelberg, Germany, 1997.
- Fischer, H., M. Werner, D. Wagenbach, M. Schwager, T. Thorsteinsson, F. Wilhelms, J. Kipfstuhl, and S. Sommer, Little Ice Age clearly recorded in northern Greenland ice cores, *Geophys. Res. Lett.*, 25(10), 1749–1752, 1998a.
- Fischer, H., D. Wagenbach, and J. Kipfstuhl, Sulfate and nitrate firm concentrations on the Greenland ice sheet, 1, Large-scale geographical deposition changes, *J. Geophys. Res.*, 103, 21,927–21,934, 1998b.
- Fischer, H., D. Wagenbach, and J. Kipfstuhl, Sulfate and nitrate firm concentrations on the Greenland ice sheet, 2, Temporal anthropogenic deposition changes, *J. Geophys. Res.*, 103, 21,935–21,942, 1998c.
- Hansson, M. E., The Renland ice core, A Northern Hemisphere record of aerosol composition over 120,000 years, *Tellus*, 46(5), 390–418, 1994.
- Hurrell, J. W., Decadal trends in the North Atlantic Oscillation: Regional temperatures and precipitation, *Science*, 269, 676–679, 1995.

- Johnsen, S. J., H. B. Clausen, W. Dansgaard, K. Fuhrer, N. Gundestrup, C. U. Hammer, P. Iversen, J. Jouzel, B. Stauffer, and J. P. Steffensen, Irregular glacial interstadials recorded in a new Greenland ice core, *Nature*, 359, 311–313, 1992.
- Kahl, J. D. W., D. A. Martinez, H. Kuhns, C. Davidson, J.-L. Jaffrezo, and J. M. Harris, Air mass trajectories to Summit, Greenland: A 44-year climatology and some episodic events, *J. Geophys. Res.*, 102, 26,861–26,876, 1997.
- Kreutz, K., P. A. Mayewski, L. D. Pittalwala, L. D. Meeker, M. S. Twickler, and S. I. Whitlow, Sea level pressure variability in the Amundsen Sea region inferred from a West Antarctic glaciochemical record, *J. Geophys. Res.*, 105, 4047–4059, 2000.
- Legrand, M. R., and R. J. Delmas, Formation of HCl in the Antarctic atmosphere, *J. Geophys. Res.*, 93(6), 1988.
- Legrand, M., A. Leopold, and F. Domine, Acidic gases (HCl, HF, HNO₃, HCOOH, and CH₃COOH): A review of ice core data and some preliminary discussions on their air-snow relationships, in *Chemical Exchange Between the Atmosphere and Polar Snow*, edited by E. W. Wolff and R. C. Bales, pp. 19–43, Springer-Verlag, New York, 1996.
- Mann, M. E., R. S. Bradley, and M. K. Hughes, Global-scale temperature patterns and climate forcing over the past six centuries, *Nature*, 392, 779–787, 1998.
- Mayewski, P. A., W. B. Lyons, M. J. Spencer, M. S. Twickler, C. F. Buck, and S. Whitlow, An ice-core record of atmospheric response to anthropogenic sulphate and nitrate, *Nature*, 346, 554–556, 1990.
- Mayewski, P. A., et al., Changes in atmospheric circulation and ocean ice cover over the North Atlantic during the last 41000 years, *Science*, 263, 1747–1751, 1994.
- Mayewski, P. A., L. D. Meeker, M. Twickler, S. Whitlow, Q. Yang, W. B. Lyons, and M. Prentice, Major features and forcing of high-latitude Northern Hemisphere atmospheric circulation using a 110,000-year-long glaciochemical series, *J. Geophys. Res.*, 102, 26,345–26,366, 1997.
- Minikin, A., D. Wagenbach, W. Graf, and J. Kipfstuhl, Spatial and seasonal variations of the snow chemistry at the central Filchner-Ronne Ice Shelf, Antarctica, *Ann. Glaciol.*, 20, 283–290, 1994.
- O'Brien, S. R., P. A. Mayewski, L. D. Meeker, D. A. Meese, M. S. Twickler, and S. I. Whitlow, Complexity of Holocene climate as reconstructed from a Greenland ice core, *Science*, 270, 1962–1964, 1995.
- Petit, J.R., et al., Climate and atmospheric history of the past 420,000 years from the Vostok ice core, Antarctica, *Nature*, 399, 429–436, 1999.
- Sommer, S., *Hochauflösende Spurenstoffuntersuchungen an Eisbohrkernen aus Nord-Grönland*, Phys. Inst., Univ. Bern, Bern, Switzerland, 1996.
- Sommer, S., D. Wagenbach, R. Mulvaney, and H. Fischer, Glacio-chemical study covering the past 2 kyr on three ice cores from Dronning Maud Land, Antarctica, 2, Seasonally resolved chemical records, *J. Geophys. Res.*, 105, 29,423–29,433, 2000.
- Steffensen, J. P., Analysis of the seasonal variation in dust, Cl⁻, NO₃⁻, and SO₄²⁻ in two central Greenland firn cores, *Ann. Glaciol.*, 10, 171–177, 1988.
- Steffensen, J. P., H. B. Clausen, and J. M. Christensen, On the spatial variability of impurity content and stable isotopic composition in recent Summit snow, in *Chemical Exchange Between the Atmosphere and Polar Snow*, edited by E. W. Wolff and R. C. Bales, pp. 607–615, Springer-Verlag, New York, 1996.
- Svensson, A., P. E. Biscaye, and F. E. Grousset, Characterization of late glacial continental dust in the Greenland Ice Core Project ice core, *J. Geophys. Res.*, 105, 4637–4656, 2000.
- Thompson, D. W. J., and J. M. Wallace, The Arctic Oscillation signature in the wintertime geopotential height and temperature fields, *Geophys. Res. Lett.*, 25(9), 1297–1300, 1998.
- van Loon, H., and J. C. Rogers, The seesaw in winter temperatures between Greenland and northern Europe, part I, General description, *Mon. Weather Rev.*, 106, 296–310, 1978.
- Wallace, J. M., and D. S. Gutzler, Teleconnections in the geopotential height field during the northern hemisphere winter, *Mon. Weather Rev.*, 109, 784–812, 1981.
- Werner, M., *Vergleichende Studie über die Verteilung vulkanogener Spurenstoffdepositionen in Nord-Ost-Grönland*, Inst. für Umweltpphys., Univ. Heidelberg, Heidelberg, Germany, 1995.
- White, J. W. C., L. K. Barlow, D. A. Fisher, P. M. Grootes, J. Jouzel, S. J. Johnsen, M. Stuiver, and H. Clausen, The climate signal in the stable isotopes of snow from Summit, Greenland: Results of comparison with modern climate observations, *J. Geophys. Res.*, 102, 26,425–26,439, 1997.
- Wilhelms, F., Measuring the conductivity and density of ice cores, *Ber. Polarforsch.*, 191, 1–224, 1996.

H. Fischer, Alfred Wegener Institute for Polar and Marine Research, Columbusstrasse, D-27568, Bremerhaven, Germany. (hufischer@awi-bremerhaven.de)

(Received November 14, 2000; revised March 26, 2001; accepted April 3, 2001.)